

## RESEARCH ARTICLE

# Midgut membrane protein BmSUH facilitates *Bombyx mori* nucleopolyhedrovirus oral infection

Yanting Liang<sup>1</sup>, Weifan Xu<sup>1</sup>, Yanyan Zhou, Yun Gao, Huan Tian, Xiaofeng Wu, Yusong Xu, Huabing Wang<sup>1</sup>\*

College of Animal Sciences, Zhejiang University, Hangzhou, China

\* These authors contributed equally to this work.

\* [wanghb@zju.edu.cn](mailto:wanghb@zju.edu.cn)



## OPEN ACCESS

**Citation:** Liang Y, Xu W, Zhou Y, Gao Y, Tian H, Wu X, et al. (2022) Midgut membrane protein BmSUH facilitates *Bombyx mori* nucleopolyhedrovirus oral infection. *PLoS Pathog* 18(11): e1010938. <https://doi.org/10.1371/journal.ppat.1010938>

**Editor:** Robert F. Kalejta, University of Wisconsin-Madison, UNITED STATES

**Received:** July 22, 2022

**Accepted:** October 19, 2022

**Published:** November 16, 2022

**Copyright:** © 2022 Liang et al. This is an open access article distributed under the terms of the [Creative Commons Attribution License](https://creativecommons.org/licenses/by/4.0/), which permits unrestricted use, distribution, and reproduction in any medium, provided the original author and source are credited.

**Data Availability Statement:** All relevant data are within the manuscript and its [Supporting Information](#) files.

**Funding:** This work was supported by the National Natural Science Foundation of China (grant no. 32170483 and 31970460 to H.B.W.), Natural Science Foundation of Zhejiang Province (grant no. LR22C040001 to H.B.W.), Zhejiang Provincial Science and Technology Plans (grant no. 2021C02072-6 to H.B.W.), and Zhejiang Provincial Key Laboratory Construction Plans (grant no.

## Abstract

Baculoviruses are virulent pathogens that infect a wide range of insects. They initiate infections via specific interactions between the structural proteins on the envelopes of occlusion-derived virions (ODVs) and the midgut cell surface receptors in hosts. However, host factors that are hijacked by baculoviruses for efficient infection remain largely unknown. In this study, we identified a membrane-associated protein sucrose hydrolase (BmSUH) as an ODV binding factor during *Bombyx mori* nucleopolyhedrovirus (BmNPV) primary infection. BmSUH was specifically expressed in the midgut microvilli where the ODV-midgut fusion happened. Knockout of BmSUH by CRISPR/Cas9 resulted in a significantly higher survival rate after BmNPV orally infection. Liquid chromatography-tandem mass spectrometry analysis and co-immunoprecipitation analysis demonstrated that PIF protein complex required for ODV binding could interact with BmSUH. Furthermore, fluorescence dequenching assay showed that the amount of ODV binding and fusion to the midgut decreased in *BmSUH* mutants compared to wild-type silkworm, suggesting the role of BmSUH as an ODV binding factor that mediates the ODV entry process. Based on a multilevel survey, the data showed that BmSUH acted as a host factor that facilitates BmNPV oral infection. More generally, this study indicated that disrupting essential protein-protein interactions required for baculovirus efficient entry may be broadly applicable to against viral infection.

## Author summary

*Baculoviridae* is a large family of pathogens that infect insects and frequently cause fatal diseases. *Bombyx mori* nucleopolyhedrovirus (BmNPV) is a major threat to the sericulture industry. Although we have learned a lot about baculoviruses over the past several decades, the detailed interaction patterns between host proteins and viral proteins that lead to infection remain underexplored. Here, we determined that BmSUH, a midgut microvilli protein, was required for the efficient oral infection of BmNPV. Our research suggests that BmSUH mediates the entry of occlusion-derived virions into the midgut epithelia by interacting with *per os* infectivity factors. According to the findings, inhibition of

2020E10025 to H.B.W). The funders had no role in study design, data collection and analysis, decision to publish, or preparation of the manuscript.

**Competing interests:** The authors have declared that no competing interests exist.

viral binding to host cells is an attractive strategy to prevent infection. This study provides an approach for preventing BmNPV infection through developing genetic resistance to viruses by using CRISPR/Cas9 system to abolish the host factors that are essential for viral entry.

## Introduction

Baculoviruses (family: *Baculoviridae*) are pathogenic viruses that infect invertebrates and represent a large group of enveloped, rod-shaped viruses with double-stranded DNA [1,2]. One hallmark of the baculovirus infection cycle is the generation of two morphologically and functionally distinct progeny phenotypes: the budded virus (BV) and the occlusion-derived virus (ODV). ODVs are enveloped virus particles embedded in a protein crystal known as occlusion body (OB) [3]. Once released from OBs under the alkaline conditions of the insect midgut, ODVs enter the epithelial cells of the midgut by binding and fusion with the membrane and initiate primary infection [4,5]. Due to the complexity of *in vivo* studies and the lack of midgut cell lines supporting ODV entry, the detailed entry mechanisms directing primary infection processes have not been addressed till date [6,7]. A group of ODV envelope proteins, termed *per os* infectivity factors (PIFs) have been found to be essential for the oral infection process as the deletion of any single PIF would lead to invalid oral infection [8]. Except PIF5, the other 8 PIFs and the homologue of AcMNPV PIF9, Bm91 act in a PIF complex [9].

Given the probable saturation of ODV binding to midgut epithelial cells, a competitive experiment suggested that particular cellular receptor(s) interacting with PIF0 were present in the midgut epithelia [10]. So far, several microvillar proteins of the midgut have been found to interact with PIF proteins. For instance, PIF0 (P74) from *Helicoverpa armigera* nucleopolyhedrovirus (HearNPV) and *Autographa californica* multicapsid nucleopolyhedrovirus (AcMNPV) binds to unknown 30 kDa and 35 kDa proteins from their hosts' brush border membrane vesicles (BBMV) [11,12]. A 97 kDa unknown protein from BBMV was also found to bind to PIF5 in *Heliothis virescens* [13]. However, the nature of these binding factors or receptor(s) on midgut epithelial cells remains unknown [7]. *Bombyx mori* nucleopolyhedrovirus (BmNPV), which belongs to *Alphabaculovirus* genus, is an exclusive pathogen of the silkworm, frequently causing grasserie disease and severe economic damage to sericulture production [14,15]. Inhibiting viral entrance into midgut cells is an attractive strategy to prevent BmNPV infection. It is of great significance to investigate the essential host factors in regulating the establishment of infection.

$\alpha$ -Glucosidase (EC 3.2.1.20) is a large family of glucoside hydrolases, whose main function is to hydrolyze glucoside bonds and release glucose as a product [16,17]. In recent years, several studies have demonstrated that  $\alpha$ -glucosidases are functionally diverse. Previous studies reported the membrane-bound  $\alpha$ -glucosidase from midgut microvilli aided pathogen invasion [18]. For instance, *Culex quinquefasciatus* maltase 1, Agm3 and Cpm1 in mosquito served as receptors of *Bacillus sphaericus* binary toxin, Bta11975 and *Bemisia tabaci*  $\alpha$ -glucosidase 1 promoted the transmission of tomato chlorosis virus [19–22]. In mammals,  $\alpha$ -glucosidases have been widely reported in facilitating the efficient infection of multiple envelope viruses, including *Dengue virus*, *Hepatitis C virus*, *Hepatitis B virus*, and *human immunodeficiency virus* [23–27]. Previous studies found that a membrane-bound  $\alpha$ -glucosidase, sucrose hydrolase (BmSUH, also known as maltase A1) showed significant expression level changes after BmNPV infection [28,29]. In addition, comparative transcriptome analysis of BmNPV-susceptible and -resistant silkworm strains showed that BmSUH exhibited novel alternative splicing

when the BmNPV-susceptible silkworm strain was exposed to BmNPV [30]. These data suggest that BmSUH may be involved in BmNPV infection process. SUH was highly expressed in the midgut of lepidopteran insects including butterflies (*Papilio xuthus*) and moth (*B. mori*, *Samia cynthia ricini*, and *Trilocho varians*) [31–33]. Previous studies have focused on its function as a sucrose hydrolase, but the extent to which BmSUH is involved in BmNPV infection process remains unexplored.

In this study, we performed a series of functional studies to characterize the role of BmSUH in BmNPV infection. We applied the CRISPR/Cas9 system to directly disrupt BmSUH and investigated its potential function during the BmNPV infection process. The liquid chromatography-mass spectrometry (LC-MS/MS) and co-immunoprecipitation (Co-IP) were employed to investigate which viral proteins interacted with BmSUH. Fluorescence-dequenching assay was used to investigate if BmSUH mediates ODV binding and fusion. The data found that BmSUH facilitated the establishment of an efficient infection in *B. mori* midgut via interacting with one or more proteins in the PIF complex. These findings suggest that BmSUH acts as a host cofactor for efficient oral infection of BmNPV.

## Results

### BmSUH is specifically expressed in the midgut at the larval stage and localized in the plasma membrane

To determine the temporal expression profiles of *BmSUH* across tissues and developmental stages in *B. mori*, we retrieved the data from SilkDB 3.0 [34]. The RNA-seq profiling revealed that the expression of *BmSUH* was specifically detected in larval midgut and mainly during the feeding stage (Fig 1A). We next investigated the expression and localization of BmSUH protein on the third day of the fifth instar (L5D3) larvae by immunoblot analysis. The result showed that BmSUH was exclusively expressed in the midgut (Fig 1B), which is consistent with *BmSUH* transcript levels (Fig 1A)[31]. A transmembrane domain of BmSUH was predicted by the TMHMM and SOSUI [31,35]. To further investigate the subcellular localization of BmSUH, we constructed PIZ-BmSUH plasmid that encoded transiently expressed BmSUH protein. BmN cells were transfected with the PIZ-BmSUH plasmid and the distribution of BmSUH was determined by immunofluorescence staining using anti-BmSUH antibody. As shown in Fig 1C, BmSUH was stained positively in the plasma membrane.

### Construction of *BmSUH* deletion mutants

To further investigate the function of *BmSUH*, we constructed *BmSUH*-knockout mutants using the CRISPR-Cas9 system. Two small guide RNAs (sgRNA) were designed to target the fifth coding-exon within the *BmSUH* gene (Fig 2A). Only the sgRNA site 1 was highly efficient. Finally, two independent types of genomic deletions were obtained, where 8 bp or 22 bp were deleted compared with the wild-type (WT) (S1 Fig). The mutation caused a complete loss of BmSUH protein expression (Fig 2B). *B. mori* midgut consists of a monolayered epithelium essentially formed by columnar and goblet cells. To precisely define the localization of BmSUH, we performed immunohistochemical staining in the midgut of silkworms. The strong signal was concentrated on apical microvilli of columnar cells, showing that BmSUH is a membrane-associated protein located in the midgut microvilli (Fig 2C). No signal was detected in two types of *BmSUH* mutants, further demonstrating a complete loss of BmSUH protein expression in these two mutants (Fig 2C).

Two *BmSUH* homozygous mutants displayed a nonlethal phenotype and produced heritable targeted mutations, showing that disruption of BmSUH had no deleterious effects on



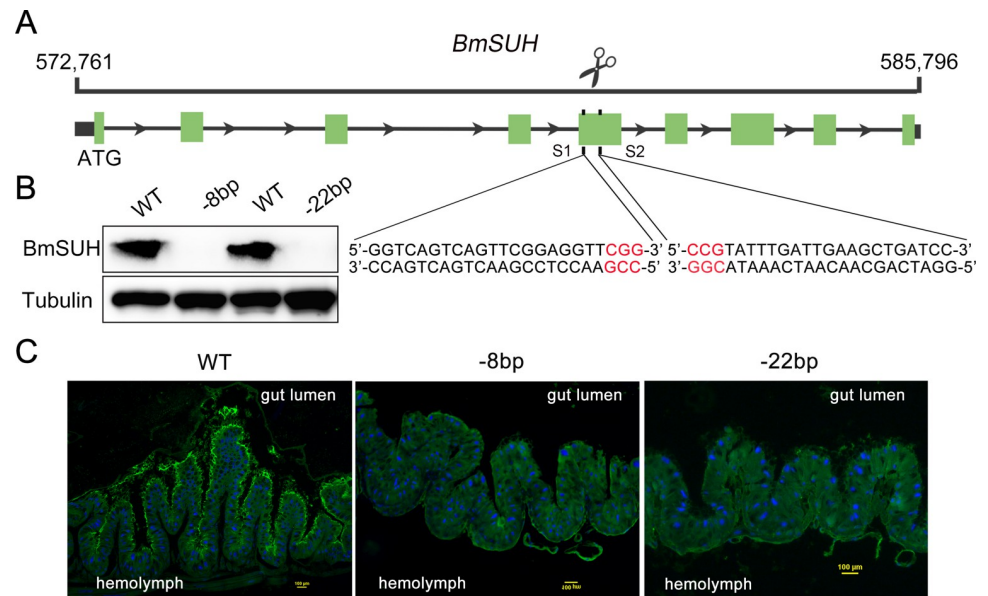


**Fig 2. Knockout of *BmSUH* in *B. mori*.** (A) Schematic description of the *BmSUH* gene and the sgRNA target site. Black and green squares represent the noncoding (UTRs) and coding parts of the transcript, respectively. The sgRNA targeting sites, S1 and S2, are located on the forward strand and reverse strand of the fifth exon, respectively. The sgRNA sequences are depicted in black and the corresponding PAM sequence is marked in red. The scissors image was obtained from the “Icon Library” of iSlide application under a CC0 1.0 Universal license. Copyright: <https://en.islide.cc/copyright-notice>. (B) Immunoblot validation of two types of *BmSUH* mutants. (C) Immunofluorescence staining of *BmSUH* (green) on midgut tissue sections of wild-type and *BmSUH* deficient silkworms. Silkworm specimens were obtained from L5D3. DAPI (blue) served as a nuclear dye. WT: wild-type; -8bp and -22bp: two *BmSUH* mutant lines.

<https://doi.org/10.1371/journal.ppat.1010938.g002>

LC50 determined in  $\Delta BmSUH$  larvae was  $3.7 \times 10^7$  OB/mL, which was 13.45-fold of that determined in WT (Table 1). Correspondingly, the percent survival of  $\Delta BmSUH$  was significantly higher than that of WT (Fig 3A). This result indicated that a higher viral dose was required to achieve lethality when *BmSUH* was deleted. We also assessed the median lethal time (LT50) by inoculating larvae with BmNPV at the concentration of  $3.48 \times 10^8$  OB/mL. The LT50 of *BmSUH* mutants was significantly longer than WT (Table 2).

To determine whether the lower mortality of  $\Delta BmSUH$  resulted from interactions of the virus with midgut cells or transfer of virus to cells in the hemocoel, we compared the virulence of BmNPV in control and mutant larvae by intrahaemocoelical injection of BV. The LD50 values of BV were  $1.56 \times 10^3$  and  $1.92 \times 10^3$  in WT and  $\Delta BmSUH$ , respectively. These results showed no significant difference between WT and  $\Delta BmSUH$  larvae (Fig 3B and Table 3). Taken together, these findings demonstrated that the absence of *BmSUH* enhanced the resistance of silkworm to BmNPV orally infection rather than BV infection, implying that *BmSUH* was mainly engaged in the midgut infective stage of primary infection.

**Table 1. LC50 of fourth instar larvae after oral infection.**

| <i>B. mori</i> | LC50 (OBs/mL)      | 95% Fiducial limit |                    |
|----------------|--------------------|--------------------|--------------------|
|                |                    | Lower              | Upper              |
| WT             | $2.75 \times 10^6$ | $1.55 \times 10^6$ | $5.09 \times 10^6$ |
| $\Delta BmSUH$ | $3.70 \times 10^7$ | $1.98 \times 10^7$ | $7.48 \times 10^7$ |

<https://doi.org/10.1371/journal.ppat.1010938.t001>

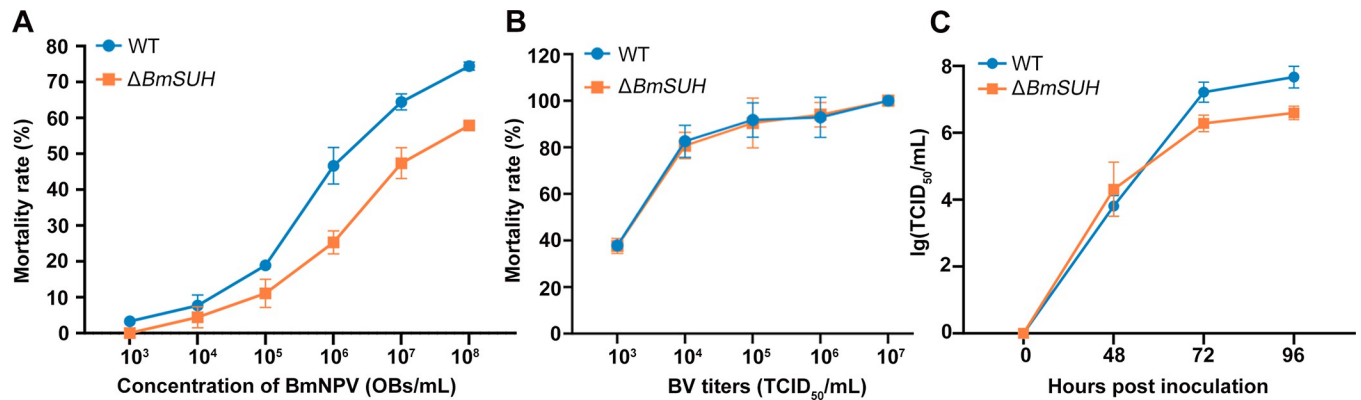


**Fig 3. Larval bioassays.** (A) The mortality analysis of fourth-instar WT and  $\Delta BmSUH$  after being orally infected with the BmNPV at concentration of  $1 \times 10^3$ ,  $1 \times 10^4$ ,  $1 \times 10^5$ ,  $1 \times 10^6$ ,  $1 \times 10^7$  and  $1 \times 10^8$  OB/mL ( $n = 30$ ). (B) The mortality of fifth-instar WT and  $\Delta BmSUH$  after BV injection ( $n = 30$ ). (C) The production of infectious BVs in the hemolymph of fourth-instar WT and  $\Delta BmSUH$  after orally infected with  $1 \times 10^8$  OB/mL BmNPV. The hemolymph was taken at designed time points and the BV titers were determined by TCID<sub>50</sub> endpoint dilution assays. Each data point was determined from the average of at least three independent experiments. The data represents the mean  $\pm$  SEM.

<https://doi.org/10.1371/journal.ppat.1010938.g003>

### BmSUH promoted the infection efficiency of BmNPV

To further explore the effect of BmSUH deletion on BV production, the hemolymph from silkworms that were orally infected with BmNPV was collected at the indicated time points. BmN cells were infected with the collected hemolymph and BV titers were determined by median tissue culture infectious dose (TCID<sub>50</sub>) endpoint dilution assay [36]. The data showed that the production of BV in WT was about 10-fold of that in  $\Delta BmSUH$  at 72 and 96 hpi (Fig 3C).

To investigate whether the absence of *BmSUH* affects the formation, assembly, and transport of virions, the midgut samples derived from the orally infected larvae at the designated time points were excised for transmission electron microscopy (TEM) analysis. A typical BmNPV infection phenomenon was observed in WT (Fig 4A). At 96 hpi, a typical electron-dense virogenic stroma (VS) was observed in the nucleus of midgut cells, and the VS contained concentrated mature viral nucleocapsids. We found nucleocapsid envelopment into intranuclear microvesicles (IM) and embedding in polyhedra (PH) at 144 hpi (Fig 4A). In contrast, the obvious VS region and abundant rod-shaped nucleocapsids were not obviously observed in the midgut of the  $\Delta BmSUH$  larvae until 144 hpi (Fig 4A). Moreover, the formation of the microvesicles and the ODV envelopment were hardly found in the midgut of  $\Delta BmSUH$  (Fig 4A). To investigate the effect of *BmSUH* deletion on viral gene expression, we selected three major viral genes that correspond to three phases of BmNPV gene temporal expression pattern: *IE1* (an immediate-early gene), *GP64* (an early-and-late gene) and *VP39* (a late gene) [37,38]. Quantitative reverse-transcription PCR (RT-qPCR) analysis revealed a significant decreased mRNA expression level of *IE1*, *GP64*, and *VP39* in  $\Delta BmSUH$  compared with that in WT at 72 and 96 hpi (Fig 4B). This result showed that the loss of BmSUH restrained the viral gene expression.

**Table 2. LT50 of fourth instar larvae after oral infection.**

| Larvae         | LT50 (h) | 95% Fiducial limit (h) |         |
|----------------|----------|------------------------|---------|
|                |          | Lower                  | Upper   |
| WT             | 96       | 91.568                 | 100.432 |
| $\Delta BmSUH$ | 108      | 104.368                | 111.632 |

<https://doi.org/10.1371/journal.ppat.1010938.t002>

**Table 3. LD50 of fifth instar larvae after BV injection.**

| <i>B. mori</i> | LD50 (TCID <sub>50</sub> ) | 95% Fiducial limit   |                      |
|----------------|----------------------------|----------------------|----------------------|
|                |                            | Lower                | Upper                |
| WT             | 1.56×10 <sup>3</sup>       | 4.3×10 <sup>2</sup>  | 3.87×10 <sup>3</sup> |
| Δ <i>BmSUH</i> | 1.92×10 <sup>3</sup>       | 5.82×10 <sup>2</sup> | 4.46×10 <sup>3</sup> |

<https://doi.org/10.1371/journal.ppat.1010938.t003>

### Identification of BmSUH-associated proteins by Co-IP and LC-MS/MS

To investigate how *BmSUH* contributes to BmNPV orally infection, we investigated viral proteins that interact with BmSUH. Midgut proteins were extracted from uninfected WT, BmNPV-infected WT and BmNPV-infected Δ*BmSUH* larvae. Then endogenous BmSUH was immunoprecipitated from the midgut extracts using the BmSUH antibody. Compared to

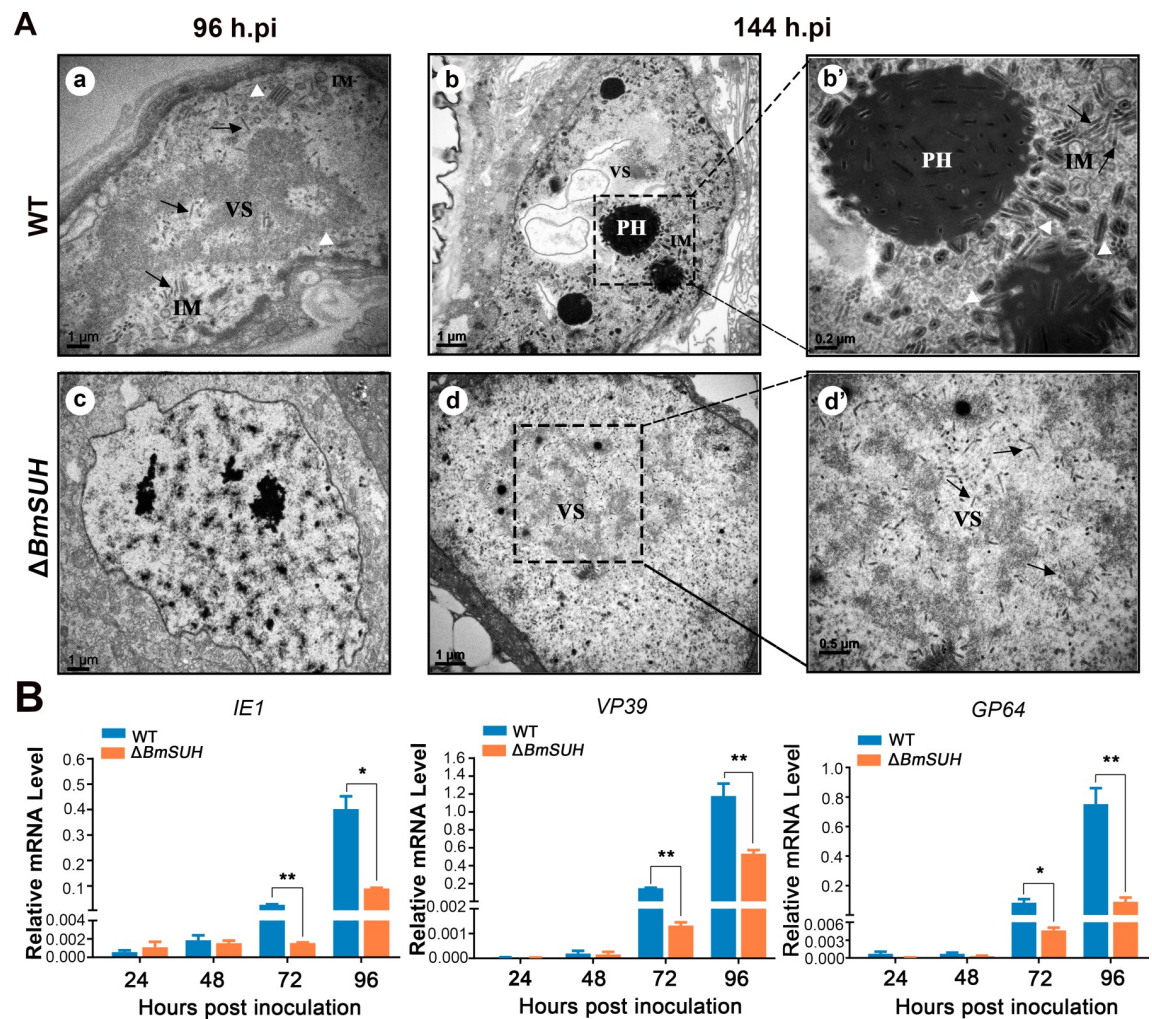


**Fig 4. Interruption of BmSUH reduced the production of virions and viral gene expression.** (A) TEM observations of virions in Δ*BmSUH* and WT larval midgut column epithelial cells. Electron-dense virogenic stroma (VS) and progeny nucleocapsids (black arrows) were observed both in the midgut of WT and Δ*BmSUH* larvae. The white triangles show intranuclear microvesicles (IM) and nucleocapsids associated with the membranous vesicular structures. PH, polyhedral. (B) Expression levels of different-phase viral genes, *IE1*, *GP64*, and *VP39* in WT or Δ*BmSUH* larvae midgut after inoculated orally with 10<sup>6</sup> OBs (mean ± SEM). \**p* < 0.05 and \*\**p* < 0.01 by two-tailed Student *t* test.

<https://doi.org/10.1371/journal.ppat.1010938.g004>

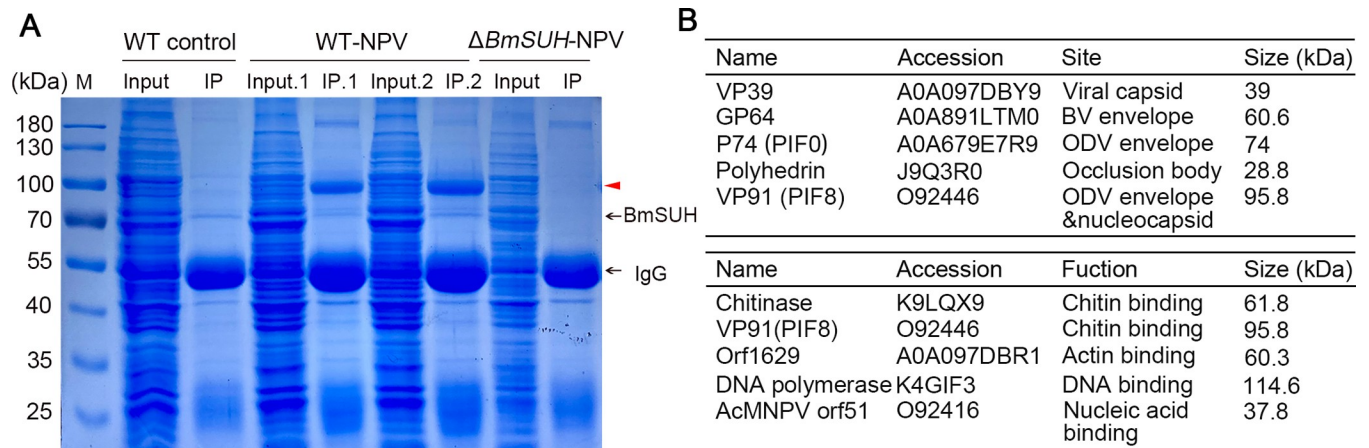


**Fig 5. Identification of BmSUH interacting proteins by LC-MS/MS analysis of endogenous CO-IP products.** (A) SDS-PAGE gel image of samples after endogenous BmSUH immunoprecipitation. Whole-cell lysates of midgut tissue were used for immunoprecipitation (IP) with anti-BmSUH. The red triangle represented the specific bands. (B) Viral proteins detected by LC-MS/MS in 70 kDa and 100 kDa gels. The structural proteins of BmNPV were shown in the upper graph and the proteins that belonged to the functional categories of “binding” in GO analysis were showed in the lower graph. IP.1: the IP sample at 72 hpi; IP.2: the IP sample at 96 hpi.

<https://doi.org/10.1371/journal.ppat.1010938.g005>

$\Delta$ BmSUH sample, two distinct bands of approximately 70 kDa and 100 kDa in WT samples were observed after BmNPV infection (Fig 5A). The 100 kDa band appeared only in BmNPV-infected WT samples, indicating that this band was a unique virus binding band (Fig 5A). To identify the viral and host proteins that were associated with BmSUH after BmNPV infection, the 70 kDa and 100 kDa bands were subjected to LC-MS/MS. A total of 631 BmSUH-associated host proteins were identified in the 100 kDa band. GO analysis revealed that the host proteins were mainly membrane associated, and predominantly enriched in molecule binding, such as small molecule binding (GO:0036094), nucleotide binding (GO:0000166), unfold-protein binding (GO:0051082) categories and so on (S5 Fig).

In addition, a total of 16 viral proteins were identified in 70 kDa and 100 kDa bands. Five of them were structural proteins of BmNPV and the others mainly belonged to the functional categories of “binding” (Fig 5B and S1 Table). The structural proteins included VP39, GP64, P74, Polyhedrin and VP91. The structural proteins form viral structures and are often required for initiating infection [39,40]. VP39 is thought to be the major capsid protein [41]. Polyhedrin is the major structural component of occlusion bodies [42]. GP64 is specific to BV envelopes, while VP91 (also known as PIF8) and P74 (also known as PIF0) are specific to ODV envelopes [7,43]. BmSUH associated with these major proteins of BmNPV in vivo, suggesting that BmSUH play an essential role during the midgut infection process.

### BmSUH interacts with PIF complex

PIFs are necessary for BmNPV orally infection but dispensable for BV infection [8]. Interestingly, two PIF proteins, PIF0 and PIF8, were detected in the LC-MS/MS result (Fig 5B). To confirm whether PIF0 and PIF8 interact with BmSUH, we performed Co-IP and reverse Co-IP assays in BmN cells as previously described [44]. The results showed that BmSUH could interact with PIF0 and PIF8 (Fig 6). Previous study found that PIF proteins act in a PIF complex, which contains PIF0, PIF1, PIF2, PIF3, PIF4, PIF6, PIF7, PIF8 and Bm91 [9]. BmSUH interacts with two components of the PIF complex, suggesting that it might be associated with the PIF complex. A series of Co-IP and reverse Co-IP assays were performed to explore whether BmSUH interacted with the PIF complex. The results showed that all components of

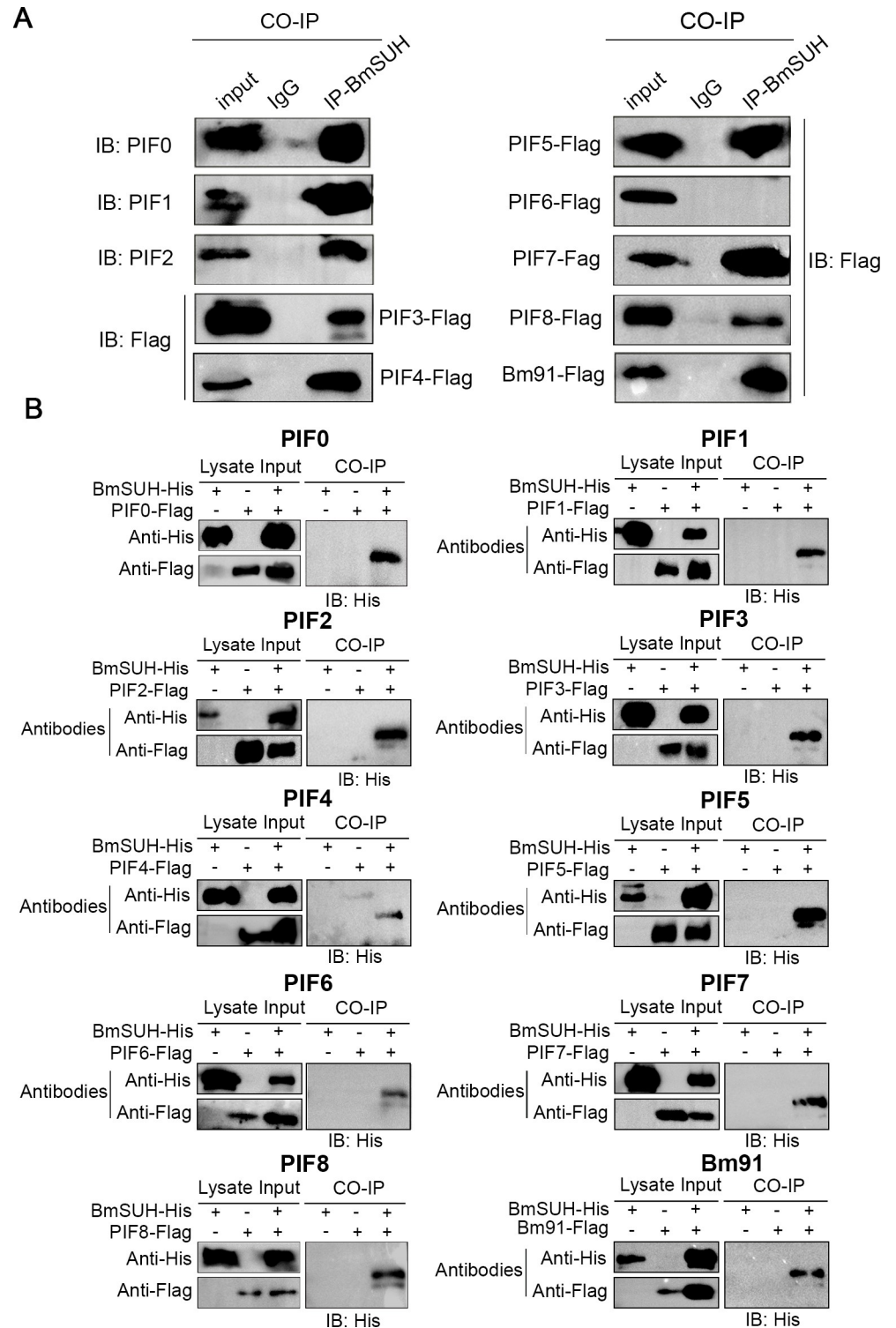


**Fig 6. Co-immunoprecipitation analysis of interactions between different PIFs and BmSUH protein.** (A) Co-IP analysis of BmSUH in NPV-infected BmN cells. BmN cells were infected with recombinant viruses expressing BmSUH-His or co-infected with BmSUH-His and PIFs-Flag. Immunoprecipitation (IP) was performed using anti-BmSUH or anti-IgG antibody followed by immunoblotting (IB) with anti-PIF0, anti-PIF1, anti-PIF2 or anti-Flag antibody individually. (B) BmN cells that were infected or co-infected with recombinant viruses expressing BmSUH-His or/and a Flag-tagged PIFs were subjected to anti-Flag. Inputs and eluates were analyzed by immunoblotting with anti-His.

<https://doi.org/10.1371/journal.ppat.1010938.g006>

the PIF complex had an interaction with BmSUH, suggesting that BmSUH interacts with the PIF complex (Fig 6). Although PIF5 was not a component of the PIF complex, it also had an interaction with BmSUH (Fig 6).

### Disruption of *BmSUH* decreased the binding and fusing efficiency of ODV with epithelial cell membranes

Previous studies demonstrated that PIFs mediated the process of ODV binding and fusing to columnar cell microvilli of midgut [6,45]. To further investigate the role of BmSUH in the initial stages of baculovirus oral infection, we performed an octadecyl rhodamine B chloride (R18) dequenching assay. This method relies upon the relief of fluorescence self-quenching of octadecyl rhodamine B chloride. We labeled ODV with a sufficiently high concentration of R18 (ODV<sub>R</sub>) to achieve self-quenching of the probe. Then we fed the ODV<sub>R</sub> to fourth instar WT and  $\Delta BmSUH$  larvae. When the ODV<sub>R</sub> fused with the midgut cell membrane, the R18 probes would diffuse into the columnar cell membrane and result in a fusion-associated fluorescence increase [46,47]. Based on this, we performed fluorescence-dequenching assays to quantify levels of ODV<sub>R</sub> attachment and fusion in the midgut of WT and  $\Delta BmSUH$  larvae. As shown in Fig 7, maximum levels of R18 were achieved within the first 30 min after inoculation, and the levels remained constant for at least 90 min after inoculation. In the WT group, the amount of bound ODV<sub>R</sub> ranged between  $0.018 \pm 0.009 \mu\text{g}$  and  $0.024 \pm 0.007 \mu\text{g}$ ; of these, approximately 55% fused ( $0.009 \pm 0.005 \mu\text{g}$  to  $0.014 \pm 0.004 \mu\text{g}$ ) (Fig 7). By comparison, the binding and fusion levels of ODV<sub>R</sub> in *BmSUH* mutants, decreased to 57% and 52% of WT, respectively (Fig 7). These results show that BmSUH is important for the process of ODV binding and fusion with host midgut epithelial cells.

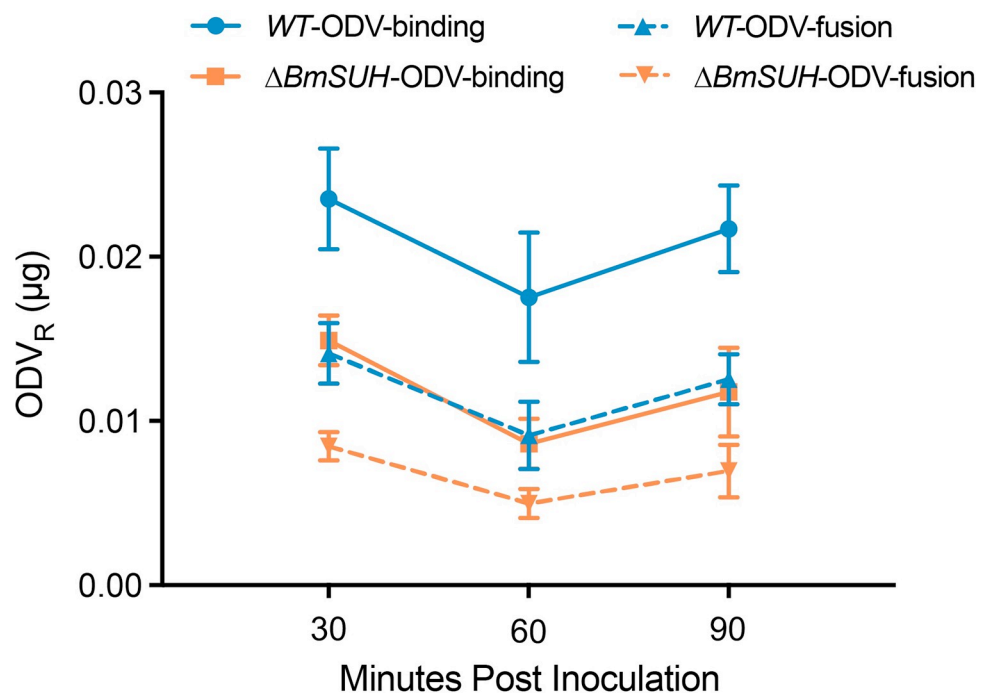


**Fig 7. The absence of BmSUH affects the interaction of ODV with midgut epithelium cells.** The amounts of labelled ODV<sub>R</sub> bound (solid line) and fused (dotted line) to the midgut epithelia of fourth-instar WT and  $\Delta BmSUH$  were detected after larvae feeding of 3  $\mu\text{g}$  of labelled ODV<sub>R</sub> from BmNPV and incubated with the designed time (n = 24, per time point). The data were analyzed using the GraphPad Prism 9 software. All data were shown as mean  $\pm$  SEM.

<https://doi.org/10.1371/journal.ppat.1010938.g007>

## Discussion

The interaction between viral attachment proteins and host cellular factors is the first and decisive step in initiating virus entry into the host cells and establishing successful infections [48]. The host proteins that facilitate ODV entry remain largely unknown. Here, we found that the midgut microvilli protein BmSUH appeared to be crucial for efficient invasion of BmNPV. BmNPV “hijacks” BmSUH to facilitate its oral infection by interacting with PIFs to promote ODV virion entry. These findings advance knowledge of the molecular mechanisms and cellular requirements of baculovirus invasion entry into the host midgut and provide a potential new strategy for preventing BmNPV infection.

BmSUH exhibited a distinctly different localization compared to a well-known sucrose-hydrolyzing enzyme, BmSUC1, which is localized in the goblet cell cavities, but a similar pattern to another membrane-bound alkaline phosphatase (mALP), whose location has been demonstrated in the apical microvilli of columnar cells [49,50]. In addition, BmSUH contains an *N*-terminal hydrophobic transmembrane region that may anchor BmSUH in the midgut microvillar membranes, which is the first area of directed contact between BmNPV and host cells after the peritrophic membrane has been penetrated. The *BmSUH* mutants developed into adulthood well without noticeable developmental problems, except a slightly delayed growth in the 5th instar compared to the control under standard feeding conditions, suggesting that BmSUH is dispensable for silkworm development but is beneficial for silkworm growth.

*BmSUH* mutants exhibit higher resistance to BmNPV *per os* infection. When the silkworms were infected by intrahemocoelic injection of BVs, which bypassed the midgut, the survival rate and LD50 had no significant differences in *BmSUH* mutants compared with WT. However, the absence of BmSUH significantly improved silkworm survival rates after being orally infected with OBs, suggesting that BmSUH plays an essential role during the BmNPV midgut infection stage of primary infection. We observed that viral assembly proceeds as normal in the midgut of  $\Delta BmSUH$ , despite the fact that the rate of polyhedron assembly was much slower. In addition, the production of BVs and the mRNA level of viral genes were significantly decreased in  $\Delta BmSUH$ . These observations suggested that BmSUH was not involved in the assembling of virions, but was rather required for virus infection efficiency. Taken together, our findings suggest that BmSUH is required for the efficient of primary infection.

Viral structural proteins are essential for viral genome protection and infection initiation but are likely not required for functions such as DNA replication [40]. The binding partners of BmSUH we identified during BmNPV infection were mainly viral structural proteins and binding proteins. These structural proteins include VP39, GP64, P74 (PIF0), Polyhedrin, and VP91 (PIF8), which are all encoded by baculovirus core genes. Among these, GP64, PIF0, and PIF8 were required for BmNPV entry. GP64 is required for BV binding to the cell surface receptors during the process of BV entry, while PIF0 and PIF8 are required for ODV to enter midgut cells [12,43,51]. The absence of BmSUH reduced infectivity of BmNPV via orally infection instead of by BV injecting. This result was consistent with the effect of deleting PIF proteins, which aborted BmNPV oral infection but the infectious remained following intrahemocoelic injection [9]. The GP64 mRNA level was significantly decreased in  $\Delta BmSUH$  after BmNPV infection. It will be interesting to explore whether the lower BV titer in *BmSUH* mutants is related to the interaction of BmSUH and GP64 in the future.

PIF-mediated entry is a commonly used and ancient entry mechanism since PIFs are highly conserved in a diverse range of viruses with large, circular, double-stranded DNA genomes that co-evolved with their hosts for millions of years [8,52–54]. BmNPV ODV entry is a complicated process that includes at least 9 PIF proteins. Except PIF5, the other 8 PIFs and Bm91 constitute all the components of a ~500 kDa PIF complex, and this complex is conserved in

BmNPV, AcMNPV, and HearNPV [9]. The PIF complex has been found to mediate ODV fusion with the plasma membrane [55]. When deleting PIF0, PIF1 or PIF2, which leads to the disappearance of the PIF complex, the ODV binding and fusing to epithelial cells are blocked (PIF0) or partly blocked (PIF1 or PIF2) [6]. Since BmSUH interacted with PIF complex, conceivably, the PIF complex might potentially mediate the ODV binding process by interacting with BmSUH. In support of this, we found that the amounts of ODV binding and fusion to midgut epithelial cells were reduced in 57% and 52% of WT in the *BmSUH* mutants, respectively. Of note, the loss of BmSUH did not ultimately abolish viral replication or gene expression, showing that the entry process is partly blocked and suggesting that ODV entry is a multistep process that may involve several cell surfaces factors (Fig 8). Although it is likely that

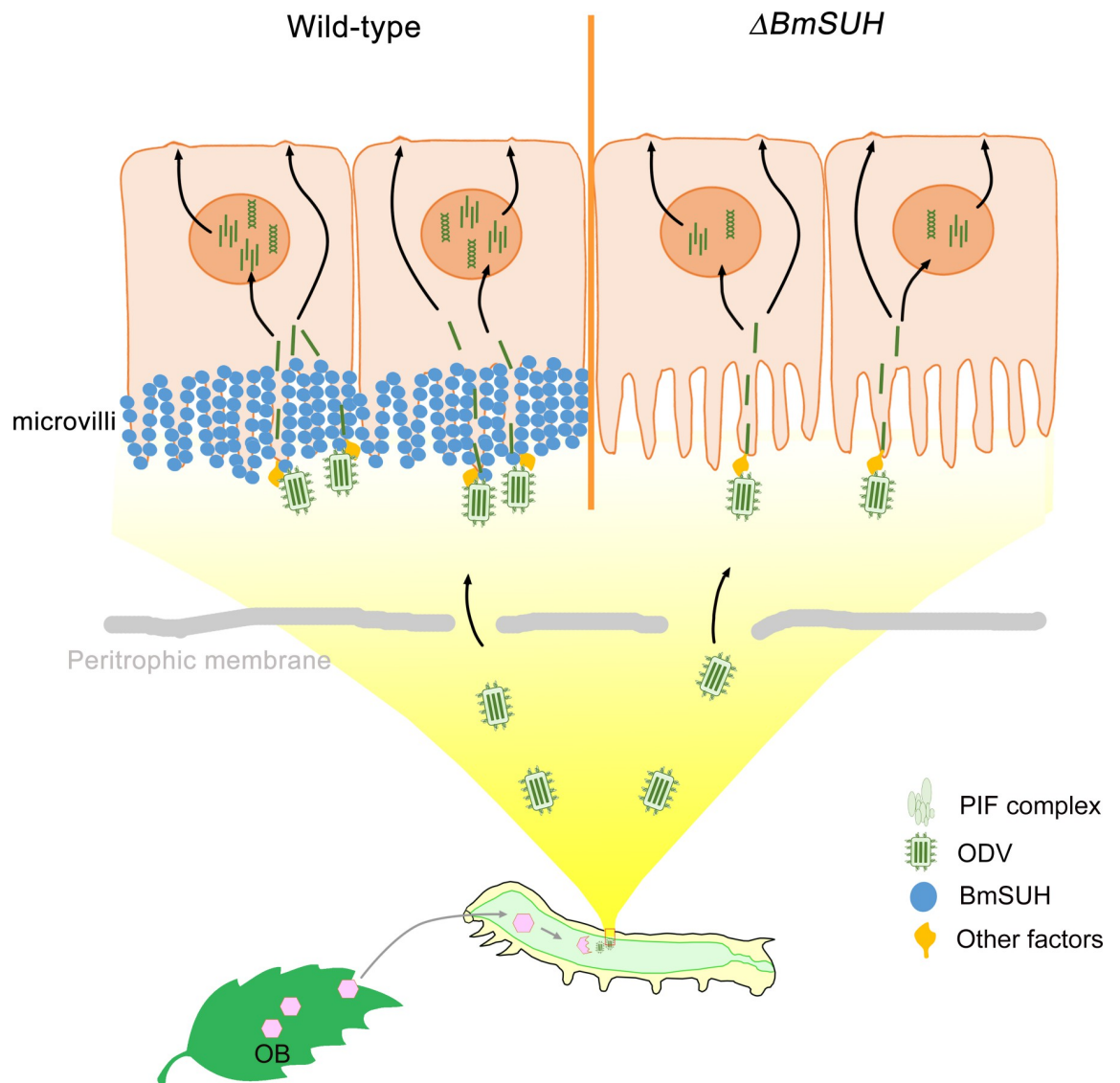


**Fig 8. Proposed model of baculovirus oral infection in wild-type or *BmSUH* mutants.** BmSUH is widely distributed in the microvilli of *Bombyx mori*. After ODV virions traverse the peritrophic membrane, PIF complex binds to BmSUH and other host factors in the microvilli of epithelial midgut cells. Then the ODV virions fuse with microvilli, releasing nucleocapsids into the cytoplasm. In *BmSUH* mutants, PIF complex could not bind to BmSUH. The loss of BmSUH reduced the ODV entry and led to a lower efficiency of oral infection (the right part). The DNA clipart was obtained from the “Icon Library” of iSlide under a CC0 1.0 Universal license. The silkworm was drawn based on a clipart obtained from the “Icon Library” of iSlide under a CC0 1.0 Universal license. Copyright: <https://en.islide.cc/copyright-notice>.

<https://doi.org/10.1371/journal.ppat.1010938.g008>

other host factors mediate in this process, our current findings show that BmSUH acts as a cofactor to enhance ODV binding and fusion to the midgut.

According to the LC-MS/MS and CO-IP results, BmSUH could interact with the PIF complex. However, it seems unlikely that all the components of the PIF complex would directly bind to BmSUH. BmSUH may facilitate BmNPV oral infection in *B. mori* midgut via interacting with one or more proteins in the PIF complex. The assembly pattern and structure of PIF complex are still unclear. Therefore, the full characterization of this BmSUH-PIF complex interaction will be of significant importance in the future. It will provide insight into the detailed molecular mechanisms of BmSUH-PIF complex mediated BmNPV entry.

The homologs of SUH have been identified in many lepidopteran species, which implies an evolutionarily conserved role of SUH in Lepidoptera [15–17]. It is worthwhile to determine whether SUH functions as the specific host factor for the BmNPV or as a general target for other NPVs in lepidopteran insects. Clearly, viruses have evolved several different strategies to use the host proteins to their own advantage [56–59]. BmSUH appears as an attractive and potential BmNPV target, for its wide distribution on the midgut epithelial microvilli. In this study, we did not observe visible damage of the midgut epithelium in *BmSUH* mutants. Even so, we cannot rule out the possibility that disruption of BmSUH may reduce BmNPV infectivity through other potential indirect ways. Although our results reveal BmSUH as an important host factor for the initial steps in BmNPV infection, the detailed mechanism of how BmSUH binds to these PIFs to assist the entry of ODV needs further exploration. In addition, this study provides a proof-of-principle for an antiviral strategy—namely, genome editing of a host protein to inhibit the interaction between ODVs and insect midgut epithelial cells required for baculovirus infection.

## Materials and methods

### Insects, cell culture, and the preparation of viral stocks

A multivoltine silkworm strain, Nistari, was maintained at our laboratory and used in this study. BmN cells were maintained in Sf-900 II SFM (Invitrogen) supplemented with 10% fetal bovine serum (Invitrogen) at 27°C as previously described [44]. The WT BmNPV is preserved in our laboratory. BmBacmid was extracted from *E. coli* strain BW25113 and used as a template. The OBs were purified from homogenized BmNPV-infected cadavers by differential centrifugation and stored at 4°C for use.

### Antibodies

The polyclonal antibodies against PIF1, PIF2 and PIF3 were gifts from Professor Zhihong Hu (Wuhan Institute of Virology, PR China) [9]. Anti-PIF0 antibody was preserved by our laboratory [60]. The anti-Flag and anti-His antibodies were purchased from HUABIO.

The anti-BmSUH antibody was prepared in our library as follows: A selected sequence (124 aa) of *BmSUH* was amplified by PCR with the primers shown in S2 Table, using cDNA of the midgut as a template. PCR products were inserted into the *Bam*H I and *Xho* I sites of the prokaryotic expression vector pCold I (TaKaRa). The recombinant plasmid pCold I-BmSUH was transformed into *E. coli* strain BL21. The truncated BmSUH protein was purified and its anti-serum was raised in rabbits.

### Construction of CRISPR/Cas9 system in *B. mori*

The Cas9 mRNA with T7 promoter was synthesized *in vitro* using a linearized plasmid as a template, following the manufacturer's instructions of the mMessage mMachine T7 Kit

(Ambion). A Poly(A) tailing kit (Ambion) was used to add the Poly(A) signals at the 3' ends of the mRNAs. The sgRNAs were customized using the online tool of ZiFit Targeter (<http://bindr.gdcb.iastate.edu/ZiFiT/>) [61]; the sequences of designed sgRNAs are listed in [S2 Table](#). The sgRNAs were prepared by transcription performed using T7 MEGAscript Kit (Ambion). Fertilized eggs within 6 hours of oviposition were microinjected with a mixture of Cas9-coding mRNA (300 ng/ $\mu$ l) and *BmSUH* sgRNA (100 ng/ $\mu$ l) [62]. The injected eggs were incubated at 25°C for 7–8 days until hatching, and the newly hatched larvae were reared with fresh mulberry leaves.

### Cas9/sgRNA-mediated mutation screens

To test Cas9/sgRNA-mediated gene alteration, sequencing and western blot were performed. Rearing the G0 generation until adulthood, the total DNA from the moth's leg was extracted and then used the PCR production for sequencing with the primer pairs ([S2 Table](#)). When the multiple sequence peaks were shown at the lower position in panel reports, representative DNA sequencing results of the PCR products from G0 moth, indicated that mutation had reduced [63]. The putative mutants of G0 adults were then crossed with WT moths to produce G1 offspring. To investigate mutations in G0 that have been germline transmitted to the G1 offspring, we sequenced the G1 generation in the same way as described previously. In order to quickly acquire homozygous, mosaic individuals for the same loci were crossed with each other [64,65]. In the meantime, the midgut was dissected, ground, lysed, and subjected to western blot using the antiserum against BmSUH. The homozygous mutant was produced when the sequence peaks were single and the signal could not be detected by western blot.

### Immunofluorescence

To investigate the specific expression pattern and localization of BmSUH, the midgut samples of WT and *BmSUH* mutant larvae at L5D3 were dissected, fixed in the paraformaldehyde (PFA) fixative, dehydrated with gradient ethanol, and infiltrated with ethanol and xylene, followed by embedding in paraffin blocks. Subsequently, the 3  $\mu$ m sections were obtained and deparaffinized with xylene, followed by rehydration with graded methanol series. After heat treatment in citrate buffer, the sections were blocked using goat serum (1:100 dilution) before incubation with the BmSUH antiserum (1:200 dilution) at 4°C overnight. Subsequently, the sections were washed with PBS and incubated with goat anti-rabbit IgG conjugated to fluorescein isothiocyanate (FITC) (1:500 dilution). Finally, the labeled sections were stained with 4',6'-diamidino-2-phenylindole (DAPI) and examined using a fluorescence microscope (NISELEMENTS; Nikon).

The Open Reading Frame of BmSUH was cloned into the PIZ/V5-His vector. The verified recombinant plasmid was extracted and marked as PIZ-BmSUH. Then the positive constructs were transfected into BmN cells using Cellfectin II (Invitrogen). After 72 h, the medium was discarded and the cells were washed twice with cold PBS. Fix cells with 4% formaldehyde for 15 minutes at 37°C. After washing cells three times in cold PBS, the cells were incubated with 1 mL 5.0  $\mu$ g/mL WGA conjugate for 10 minutes at room temperature. The cells were washed three times in cold PBS. The following procedures were the same as the immunofluorescence staining mentioned above. Finally, the cells were observed under a Zeiss LSM780 laser-scanning confocal microscope.

### Larval bioassays

To determine the LC50 and LD50, for one set, the newly molted fourth-instar larvae of WT and BmSUH mutants were starved for 12 h and then fed with 10  $\mu$ L different concentrations

of BmNPV ( $1 \times 10^3$  to  $1 \times 10^8$  of OB/mL). For the other set, the LD50 was determined in fifth-instar WT and BmSUH mutant silkworms by haemocoelic injection with different doses of BV diluted in Sf-900 II SFM medium. Each group contained 30 silkworm larvae, and three independent experiments were carried out as biological replicates. Probit analysis of mortality data was conducted using SPSS v.26.0 software (IBM).

For LT50, newly molted fourth-instar larvae including *BmSUH* mutants and WT were starved for 12 h. Each larva was fed with a 1 cm<sup>2</sup> piece of mulberry leaf smeared with 10  $\mu$ L OBs at the concentration of  $3.48 \times 10^8$  OB/mL. Only larvae that consumed the entire leaf piece were maintained and were reared individually with fresh mulberry leaves. Virus-induced mortality was recorded every 12 h until insect death or pupation. Bioassays with 30 larvae were performed in triplicates. The Kaplan-Meier estimator was applied to evaluate the LT<sub>50</sub> value using SPSS v.26.0 software (IBM).

To measure the BV production, the hemolymph from fourth instar silkworms that were infected with 10  $\mu$ L BmNPV at the concentration of  $1 \times 10^8$  OB/mL was collected at 48, 72 and 96 hpi. The hemolymph was filtered with 0.45  $\mu$ m filter membrane before infecting BmN cells. Infectious BV titers were determined by the median tissue culture infectious dose (TCID<sub>50</sub>) end point dilution assay as described [36].

## TEM analyses

To compare the structure of the midgut epithelium of WT and  $\Delta BmSUH$ , the midgut of L5D3 was dissected. To observe the virus in the midgut of WT and  $\Delta BmSUH$ , the fourth-instar *B. mori* larvae of WT and  $\Delta BmSUH$  were inoculated orally with  $10^6$  OBs. The midgut of each larva was dissected at 96 and 144 hpi. The cropped samples were fixed with 2.5% (v/v) glutaraldehyde overnight at 4°C and ultrathin sections were prepared for TEM (HITACHI H-7650) examination at a 100 kV accelerating voltage.

## Quantitative reverse-transcription PCR

To evaluate the effects of BmSUH protein on viral gene expression, fourth-instar WT and  $\Delta BmSUH$  larvae were inoculated orally with  $10^6$  OBs. Total RNA was extracted from WT and  $\Delta BmSUH$  larval midgut using RNAiso Plus (TaKaRa). A PrimeScript RT Reagent Kit with gDNA Eraser (TaKaRa) was used to synthesize cDNA from the extracted RNA. Quantitative mRNA measurements were performed using the TB Green Premix Ex Taq (TaKaRa) on an ABI 7300 Real-Time PCR System (Applied Biosystems). The primer sequences are listed in [S2 Table](#). The data were normalized to *B. mori* ribosomal protein 49 (Bmrp49) and analyzed with GraphPad Prism v.7.0 with the  $2^{-\Delta\Delta Ct}$  method. Two-tailed Student *t* test was used to determine significant differences between different groups of qPCR data. All data were shown as mean  $\pm$  SEM (N = 3). All assays were carried out in triplicates.

## The generation of recombinant baculoviruses expressing BmSUH and PIFs

Complete DNA encoding *BmSUH*, nine *PIFs* and *Bm91* were amplified with specific primers ([S2 Table](#)) using the cDNA of the *B. mori* midgut and BmBacmid as templates, respectively. PCR products were subcloned into pFastBac1 donor plasmid. The recombinant bacmids were constructed according to the protocol of Bac-to-Bac baculovirus expression system (Invitrogen). The recombinant bacmids were transfected into BmN cells using Lipofectamine 3000 Transfection Kit (Invitrogen) to generate recombinant baculovirus. His-tagged BmSUH (BmSUH-His) and Flag-tagged PIFs (PIFs-Flag) were expressed in baculovirus-transformed BmN cells at 27°C and harvested after four days' post-infection. The BmSUH-His and

PIF-Flag containing viral supernatants were also collected and stored at 4°C for use in the co-immunoprecipitation assay.

### Co-immunoprecipitation assay and western blot analysis

To prepare the samples for LC-MS/MS analysis, the CO-IP were performed by using midgut tissue from virus infected and uninfected larvae. The midgut tissues were lysed in 1 ml of IP buffer [20mM Tris (pH7.5), 150mM NaCl, 1% Triton X-100, 1mM PMSF] (Beyotime, Biotechnology). Lysates were centrifuged at 12,000 × g for 5 minutes at 4°C. One-tenth volumes of the supernatants were preserved as the input controls, and the rest lysates incubated at 4°C overnight with anti-BmSUH antibody. Protein A+G agarose (Beyotime Biotechnology) were added to the lysate solution for the last 4 h of incubation. At last, the agaroses were washed four times with the IP lysis buffer and then boiled in 1× SDS sample buffer containing β-mercaptoethanol.

To confirm the interaction of PIF proteins with BmSUH, we carried out two sets of in vitro CO-IP in BmN cells. The BmN cells were infected or co-infected by the BmSUH-His and PIF-Flag viruses at an M.O.I. of 5, after which infected cells were collected at 72 hpi and washed twice with 1×PBS. The collected cells were lysed in Western and IP buffer as described above. For one set of lysates, the CO-IP was performed using protein A+G agarose as described above. Western blot analyses were conducted after separation by SDS-polyacrylamide gel electrophoresis (PAGE) and transfer to a PVDF membrane. The primary antibodies used were anti-P74 (1:500 dilution), anti-PIF1 (1: 2,000 dilution), anti- and anti-PIF2 (1:2,000 dilution) and anti-Flag antibody (1:5,000 dilution).

Another set of lysates were incubated with anti-Flag Immunomagnetic Beads (Bimake) at 4°C overnight. After that, the beads were boiled in 1× SDS sample buffer and subjected to SDS- PAGE and examined by western blot. anti-Flag antibody to detect the expression and immunoprecipitation of the Flag-tagged proteins and anti-His antibody to determine if BmSUH was co-immunoprecipitated with the PIFs.

### LC-MS/MS analysis

The IP protein samples were separated by SDS-PAGE until the dye front reached the bottom of the gel. After staining with Coomassie Brilliant Blue the 70kDa and 100kDa bands were excised and subjected to LC-MS/MS analysis by Q Exactive mass spectrometer. The experiment and data analysis were supported by Shanghai Applied Protein Technology.

GO analysis was performed on the proteins identified by LC-MS/MS. The R package "TopGO" was used to analyze the GO enrichment, and the R package "ggplot" was used to visualize the results.

### Fluorescence-dequenching assay

To determine the role of *BmSUH* in viral invasion of midgut epithelial cells, fluorescence-dequenching assays were performed. To prepare ODVs, supernatants of OB lysates were purified by ultracentrifugation through 30%–60% (w/v) sucrose as previously described [60]. Subsequently, the purified ODV was labeled with the self-quenching fluorescent probe octadecyl rhodamine B chloride (R18; Invitrogen Life Technologies), as described previously [10]. Labeled ODV<sub>R</sub> was quantified using BCA protein Assay Kit (Takara) and stored in the dark at 4°C until use. Newly molted fourth-instar WT and  $\Delta BmSUH$  larvae were inoculated orally with 3 μg labeled ODV<sub>R</sub> (n = 24 larvae) or PBS (n = 24 larvae). At 30-, 60-, and 90-min post-inoculation, after which the midgut of each larva was dissected and rinsed in 200 μL chilled separation buffer (100 mM NaCO<sub>3</sub>, 100 mM KCl, 100 mM EGTA, pH 9.5) and stored in the

dark at  $-80^{\circ}\text{C}$  until use. The amounts of ODV bound and fused were measured using FLUOR-OMAX-4 fluorescence spectrophotometer (Horiba Jobin Yvon) at excitation/emission wavelengths of 560nm/583nm, after which the relative fluorescence units per mg ODV<sub>R</sub> protein was calculated.

## Supporting information

**S1 Fig. The sequence results of WT and homozygote mutant silkworm.** The target site location was shown in green and PAM sequences were shown in red. The black underlines highlight the target site location and the nearby sequences. (A) The chromatograms of WT. (B) Representative chromatograms of homozygotes. The deletion sequences were shown in gray, and the cutting site was indicated by a red arrow. (C) The mutation events were confirmed by sequencing.

(TIF)

**S2 Fig. The *BmSUH* mutants have no significant defects in fecundity and viability.** (A) Images of the eggs produced by WT and *BmSUH* mutants ( $n = 20$  couples per group). (B) The number of eggs (left panel) and the hatching rate of WT and  $\Delta BmSUH$  (right panel). Data were presented as mean  $\pm$  SD and analyzed by SPSS v.26.0 software using two-tailed Student *t* test. ns,  $P > 0.05$ .

(TIF)

**S3 Fig. TEM observation of midgut columnar cells in wild-type and *BmSUH* mutants.** Silkworm specimens were obtained from day 3 of the 5th instar (L5D3) larval. N: nucleus, M: microvilli. The white triangle indicates mitochondria, and the black arrow indicates the microapocrine vesicles.

(TIF)

**S4 Fig. BmSUH was responsive to BmNPV.** (A) Western blot analysis of BmSUH protein level in *B. mori* before and after BmNPV oral infection. Anti-tubulin was used as an internal control. (B) Quantification of western signal as the mean  $\pm$ SD ( $n = 3$  biological replicates). Signals were quantitated using Image J software. \*\* $p < 0.01$  and \*\*\* $p < 0.001$  by two-tailed Student *t* test.

(TIF)

**S5 Fig. The GO enrichment analysis of the binding partners of BmSUH.** Midgut proteins of 100 kDa gel which appeared after BmNPV infection were detected by LC-MS/MS. The identified genes were submitted to GO enrichment analysis. BP: Biological process, CC: Cellular component, MF: Molecular function.

(TIF)

**S1 Table. Viral proteins detected by LC-MS/MS following IP using anti-BmSUH.**

(XLSX)

**S2 Table. The primers used in this study.**

(XLSX)

## Acknowledgments

We thank Zhihua Hao for helpful suggestions on this study. We are grateful to Professor Boxiong Zhong, who provides practical advice on microinjection. We thank Yang Li for technical support.

## Author Contributions

**Conceptualization:** Yanting Liang, Weifan Xu, Huabing Wang.

**Data curation:** Yanting Liang, Weifan Xu, Huabing Wang.

**Formal analysis:** Yanting Liang, Weifan Xu.

**Funding acquisition:** Huabing Wang.

**Investigation:** Yanting Liang, Weifan Xu, Yanyan Zhou, Yun Gao, Huan Tian.

**Methodology:** Yanting Liang, Weifan Xu.

**Project administration:** Xiaofeng Wu, Yusong Xu, Huabing Wang.

**Resources:** Yanting Liang, Weifan Xu, Yanyan Zhou, Yun Gao, Yusong Xu, Huabing Wang.

**Supervision:** Xiaofeng Wu, Yusong Xu, Huabing Wang.

**Validation:** Yanting Liang, Weifan Xu, Huan Tian.

**Visualization:** Yanting Liang, Weifan Xu, Yanyan Zhou.

**Writing – original draft:** Yanting Liang, Weifan Xu.

**Writing – review & editing:** Yanting Liang, Weifan Xu, Huabing Wang.

## References

1. Herniou EA, Olszewski JA, Cory JS, O'Reilly DR. The genome sequence and evolution of baculoviruses. *Annu Rev Entomol.* 2003; 48:211–234. <https://doi.org/10.1146/annurev.ento.48.091801.112756> PMID: 12414741
2. Jehle JA, Blissard GW, Bonning BC, Cory JS, Herniou EA, Rohrmann GF, et al. On the classification and nomenclature of baculoviruses: a proposal for revision. *Arch Virol.* 2006; 151(7):1257–66. <https://doi.org/10.1007/s00705-006-0763-6> PMID: 16648963
3. Peng K, van Oers MM, Hu Z, van Lent JW, Vlaskovic JM. Baculovirus *per os* infectivity factors form a complex on the surface of occlusion-derived virus. *J Virol.* 2010; 84(18):9497–9504. <https://doi.org/10.1128/jvi.00812-10> PMID: 20610731
4. Elder BD, Heitman J. Developing models of disease transmission: insights from ecological studies of insects and their baculoviruses. *PLoS Pathog.* 2013; 9(6):e1003372. <https://doi.org/10.1371/journal.ppat.1003372> PMID: 23785277
5. Kawanishi CY, Summers MD, Stoltz DB, Arnott HJ. Entry of an insect virus in vivo by fusion of viral envelope and microvillus membrane. *J Invertebr Pathol.* 1972; 20(1):104–108. [https://doi.org/10.1016/0022-2011\(72\)90088-2](https://doi.org/10.1016/0022-2011(72)90088-2) PMID: 5044280
6. Mu J, van Lent JWM, Smagghe G, Wang Y, Chen X, Vlaskovic JM, et al. Live imaging of baculovirus infection of midgut epithelium cells: a functional assay of *per os* infectivity factors. *J Gen Virol.* 2014; 95(11):2531–2539. <https://doi.org/10.1099/vir.0.068262-0>
7. Blissard GW, A. TD. Baculovirus entry and egress from insect cells. *Annu Rev Virol.* 2018; 5(1):113–119. <https://doi.org/10.1146/annurev-virology-092917-043356> PMID: 30004832
8. Boogaard B, Van Oers M, Lent J. An advanced view on baculovirus *per os* infectivity factors. *Insects.* 2018; 9:84. <https://doi.org/10.3390/insects9030084> PMID: 30018247
9. Wang X, Shang Y, Chen C, Liu S, Chang M, Zhang N, et al. Baculovirus *per os* infectivity factor complex: components and assembly. *J Virol.* 2019; 93(6):e02053–18. <https://doi.org/10.1128/jvi.02053-18> PMID: 30602603
10. Haas-Stapleton EJ, Washburn JO, Volkman LE. *Autographa californica* M nucleopolyhedrovirus occlusion-derived virus to primary cellular targets in the midgut epithelia of *Heliothis virescens* Larvae. *J Virol.* 2004; 78(13):6786–6791. <https://doi.org/10.1128/JVI.78.13.6786-6791>
11. Yao L, Zhou W, Xu H, Zheng Y, Qi Y. The *Heliothis armigera* single nucleocapsid nucleopolyhedrovirus envelope protein P74 is required for infection of the host midgut. *Virus Res.* 2004; 104(2):111–121. <https://doi.org/10.1016/j.virusres>

12. Zhou W, Yao L, Xu H, Yan F, Qi Y. The function of envelope protein P74 from *Autographa californica* multiple nucleopolyhedrovirus in primary infection to host. *Virus genes*. 2005; 30(2):139–150. <https://doi.org/10.1007/s11262-004-5623-4> PMID: 15744572
13. Sparks WO, Harrison RL, Bonning BC. *Autographa californica* multiple nucleopolyhedrovirus ODV-E56 is a *per os* infectivity factor, but is not essential for binding and fusion of occlusion-derived virus to the host midgut. *Virology*. 2011; 409(1):69–76. <https://doi.org/10.1016/j.virol.2010.09.027> PMID: 20970820
14. Jiang L, Xia Q. The progress and future of enhancing antiviral capacity by transgenic technology in the silkworm *Bombyx mori*. *Insect Biochem Mol Biol*. 2014; 48:1–7. <https://doi.org/10.1016/j.ibmb.2014.02.003> PMID: 24561307
15. Khurad AM, Mahulikar A, Rathod MK, Rai MM, Kanginakudru S, Nagaraju J. Vertical transmission of nucleopolyhedrovirus in the silkworm, *Bombyx mori* L. *J Invertebr Pathol*. 2004; 87(1):8–15. <https://doi.org/10.1016/j.jip.2004.05.008> PMID: 15491594
16. Garcia-Gonzalez M, Minguet-Lobato M, Plou FJ, Fernandez-Lobato M. Molecular characterization and heterologous expression of two  $\alpha$ -glucosidases from *Metschnikowia* spp, both producers of honey sugars. *Microb Cell Fact*. 2020; 19(1):140. <https://doi.org/10.1186/s12934-020-01397-y> PMID: 32652991
17. Ojima T, Saburi W, Yamamoto T, Kudo T. Characterization of *Halomonas* sp. strain H11  $\alpha$ -glucosidase activated by monovalent cations and its application for efficient synthesis of  $\alpha$ -D-glucosylglycerol. *Appl Environ Microbiol*. 2012; 78(6):1836–1845. <https://doi.org/10.1128/AEM.07514-11> PMID: 22226947
18. Terra WR, Ferreira C. 11—Biochemistry and Molecular Biology of Digestion. In: Gilbert LI, editor. *Insect Molecular Biology and Biochemistry*. San Diego: Academic Press; 2012. pp. 365–418.
19. Guo Q-y Cai Q-x, Yan J-p Hu X-m, Zheng D-s Yuan Z-m. Single nucleotide deletion of *cqm1* gene results in the development of resistance to *Bacillus sphaericus* in *Culex quinquefasciatus*. *J Insect Physiol*. 2013; 59(9):967–73. <https://doi.org/10.1016/j.jinsphys.2013.07.002> PMID: 23871751
20. Opota O, Charles J-F, Warot S, Pauron D, Darboux I. Identification and characterization of the receptor for the *Bacillus sphaericus* binary toxin in the malaria vector mosquito, *Anopheles gambiae*. *Comp Biochem Physiol B Biochem Mol Biol*. 2008; 149(3):419–27. <https://doi.org/10.1016/j.cbpb.2007.11.002> PMID: 18086545
21. Darboux I, Nielsen-LeRoux C, Charles J-F, Pauron D. The receptor of *Bacillus sphaericus* binary toxin in *Culex pipiens* (Diptera: Culicidae) midgut: molecular cloning and expression. *Insect Biochem Mol Biol*. 2001; 31(10):981–990. [https://doi.org/10.1016/S0965-1748\(01\)00046-7](https://doi.org/10.1016/S0965-1748(01)00046-7)
22. Lu D, Yue H, Huang L, Zhang D, Zhang Z, Zhang Z, et al. Suppression of Bta11975, an  $\alpha$ -glucosidase, by RNA interference reduces transmission of tomato chlorosis virus by *Bemisia tabaci*. *Pest Management Science*. 2021; 77(11):5294–303. <https://doi.org/10.1002/ps.6572> PMID: 34310017
23. Caputo Alessandro T, Alonzi Dominic S, Marti L, Reca I-B, Kiappes JL, Struwe Weston B, et al. Structures of mammalian ER  $\alpha$ -glucosidase II capture the binding modes of broad-spectrum iminosugar antivirals. *J Clin Periodontol*. 2016; 113(32):E4630–E4638. <https://doi.org/10.1073/pnas.1604463113> PMID: 27462106
24. Tchankouo-Nguetcheu S, Khun H, Pincet L, Roux P, Bahut M, Huerre M, et al. Differential protein modulation in midguts of *Aedes aegypti* infected with chikungunya and *dengue 2* viruses. *PLoS one*. 2010; 5(10):e13149. <https://doi.org/10.1371/journal.pone.0013149> PMID: 20957153
25. Cynthia Chapel, Céline Garcia, Philippe Roingear, et al. Antiviral effect of  $\alpha$ -glucosidase inhibitors on viral morphogenesis and binding properties of hepatitis C virus-like particles. *J Gen Virol*. 2006; 87(Pt 4):861–871. <https://doi.org/10.1099/vir.0.81503-0>
26. Lu X, Mehta A, Dwek R, Butters T, Block T. Evidence That N-Linked glycosylation is necessary for *Hepatitis B Virus* secretion. *Virology*. 1995; 213(2):660–665. <https://doi.org/10.1006/viro.1995.0038> PMID: 7491790
27. Miller JL, Tyrrell BE, Zitzmann N. Mechanisms of antiviral activity of iminosugars against *dengue virus*. *Adv Exp Med Biol*. 2018; 1062:277–301. [https://doi.org/10.1007/978-981-10-8727-1\\_20](https://doi.org/10.1007/978-981-10-8727-1_20) PMID: 29845540
28. Huang H, Wu P, Zhang S, Shang Q, Yin H, Hou Q, et al. DNA methylomes and transcriptomes analysis reveal implication of host DNA methylation machinery in BmNPV proliferation in *Bombyx mori*. *BMC Genomics*. 2019; 20(1):736. <https://doi.org/10.1186/s12864-019-6146-7> PMID: 31615392
29. Zhang Y, Xia D, Zhao Q, Zhang G, Zhang Y, Qiu Z, et al. Label-free proteomic analysis of silkworm midgut infected by *Bombyx mori nuclear polyhedrosis virus*. *J Proteomics*. 2019; 200:40–50. <https://doi.org/10.1016/j.jprot.2019.03.011> PMID: 30904731
30. Gang Kaiyue, Zhou Guodong, Zhao Heying, et al. Transcriptome-wide analysis of the difference of alternative splicing in susceptible and resistant silkworm strains after BmNPV infection. *3 Biotech*. 2019; 9(4):152. <https://doi.org/10.1007/s13205-019-1669-9> PMID: 30944799

31. Wang H, Kiuchi T, Katsuma S, Shimada T. A novel sucrose hydrolase from the bombycoid silkworms *Bombyx mori*, *Trilocho varians*, and *Samia cynthia ricini* with a substrate specificity for sucrose. *Insect Biochem Mol Biol*. 2015; 61:46–52. <https://doi.org/10.1016/j.ibmb.2015.04.005> PMID: 25937576
32. Dai X, Li R, Li X, Liang Y, Gao Y, Xu Y, et al. Gene duplication and subsequent functional diversification of sucrose hydrolase in *Papilio xuthus*. *Insect Mol Biol*. 2019; 28(6):862–872. <https://doi.org/10.1111/imb.12603> PMID: 31155808
33. Li X, Shi L, Zhou Y, Xie H, Dai X, Li R, et al. Molecular evolutionary mechanisms driving functional diversification of  $\alpha$ -glucosidase in Lepidoptera. *Sci Rep*. 2017; 7(1):45787. <https://doi.org/10.1038/srep45787> PMID: 28401928
34. Lu F, Wei Z, Luo Y, Guo H, Zhang G, Xia Q, et al. SilkDB 3.0: visualizing and exploring multiple levels of data for silkworm. *Nucleic Acids Res*. 2020; 48(D1):D749–D55. <https://doi.org/10.1093/nar/gkz919> PMID: 31642484
35. Miyazaki T, Park EY. Structure–function analysis of silkworm sucrose hydrolase uncovers the mechanism of substrate specificity in GH13 subfamily 17 exo- $\alpha$ -glucosidases. *J Biol Chem*. 2020; 295(26):8784–97. <https://doi.org/10.1074/jbc.RA120.013595> PMID: 32381508
36. Hammock B. The baculovirus expression system: a laboratory guide. *Annals of the Entomological Society of America*. 1992;(4):510–511.
37. Chen S, Hou C, Bi H, Wang Y, Xu J, Li M, et al. Transgenic clustered regularly interspaced short palindromic Repeat/Cas9-mediated viral gene targeting for antiviral therapy of *Bombyx mori* Nucleopolyhedrovirus. *J Virol*. 2017; 91(8):e02465–16. <https://doi.org/10.1128/JVI.02465-16> PMID: 28122981
38. Qiu J, Tang Z, Cai Y, Wu W, Yuan M, Yang K. The *Autographa californica* Multiple Nucleopolyhedrovirus *ac51* gene is required for efficient nuclear egress of nucleocapsids and is essential for in vivo virulence. *J Virol*. 2019; 93(3):e01923–18. <https://doi.org/10.1128/JVI.01923-18> PMID: 30429334
39. Shan C, Xie X, Muruato AE, Rossi SL, Roundy CM, Azar SR, et al. An Infectious cDNA Clone of Zika Virus to Study Viral Virulence, Mosquito Transmission, and Antiviral Inhibitors. *Cell Host Microbe*. 2016; 19(6):891–900. <https://doi.org/10.1016/j.chom.2016.05.004> PMID: 27198478
40. Rohrmann GF. Structural proteins of baculovirus occlusion bodies and virions. In: *Baculovirus Molecular Biology*. Bethesda: National Center for Biotechnology Information (US); 2019. Available from: <https://www.ncbi.nlm.nih.gov/books/NBK543455/>
41. Wang R, Deng F, Hou D, Zhao Y, Guo L, Wang H, et al. Proteomics of the *Autographa californica* nucleopolyhedrovirus budded virions. *J Virol*. 2010; 84(14):7233–42. <https://doi.org/10.1128/JVI.00040-10> PMID: 20444894
42. Slack J, Arif BM. The baculovirus occlusion-derived virus: virion structure and function. *Adv Virus Res*. 2007; 69:99–165. [https://doi.org/10.1016/S0065-3527\(06\)69003-9](https://doi.org/10.1016/S0065-3527(06)69003-9) PMID: 17222693
43. Zhu S, Wang W, Wang Y, Yuan M, Yang K. The baculovirus core gene *ac83* is required for nucleocapsid assembly and *per os* infectivity of *Autographa californica* nucleopolyhedrovirus. *J Virol*. 2013; 87(19):10573–10586. <https://doi.org/10.1128/jvi.01207-13> PMID: 23864639
44. Xu W, Wang H, Liu H, Wu X. *Bombyx mori* nucleopolyhedrovirus F-like protein Bm14 is a cofactor for GP64-mediated efficient infection via forming a complex on the envelope of budded virus. *Virology*. 2020; 539:61–68. <https://doi.org/10.1016/j.virol.2019.10.008> PMID: 31678757
45. Haas-Stapleton EJ, Washburn JO, Volkman LE. P74 mediates specific binding of *Autographa californica* M nucleopolyhedrovirus occlusion-derived virus to primary cellular targets in the midgut epithelia of *Heliothis virescens* larvae. *J. Virol*. 2004; 78:6786–6791. <https://doi.org/10.1128/JVI.78.13.6786-6791.2004>
46. Tang W, Li M, Liu Y, Liang N, Yang Z, Zhao Y, et al. Small molecule inhibits respiratory syncytial virus entry and infection by blocking the interaction of the viral fusion protein with the cell membrane. *FASEB J*. 2019; 33(3):4287–4299. <https://doi.org/10.1096/fj.201800579R> PMID: 30571312
47. Sakai T, Ohuchi M, Imai M, Mizuno T, Kawasaki K, Kuroda K, et al. Dual wavelength imaging allows analysis of membrane fusion of influenza virus inside cells. *J Virol*. 2006; 80(4):2013–2018. <https://doi.org/10.1128/JVI.80.4.2013-2018.2006> PMID: 16439557
48. Barrass SV, Butcher SJ. Advances in high-throughput methods for the identification of virus receptors. *Med Microbiol Immunol*. 2020; 209(3):309–323. <https://doi.org/10.1007/s00430-019-00653-2> PMID: 31865406
49. Daimon T, Taguchi T, Meng Y, Katsuma S, Mita K, Shimada T.  $\beta$ -Fructofuranosidase genes of the silkworm, *Bombyx mori*: Insights into enzymatic adaptation of *B. mori* to toxic alkaloids in mulberry latex. *J Biol Chem*. 2008; 283:15271–15279. <https://doi.org/10.1074/jbc.M709350200> PMID: 18397891
50. Azuma M, Eguchi M. Discrete localization of distinct alkaline phosphatase isozymes in the cell surface of silkworm midgut epithelium. *Journal of Experimental Zoology*. 1989; 251(1):108–112. <https://doi.org/10.1002/jez.1402510113>

51. Zhou J, Blissard GW. Identification of a GP64 subdomain involved in receptor binding by budded virions of the baculovirus *Autographica californica multicapsid* nucleopolyhedrovirus. *J Virol*. 2008; 82(9):4449–4460. <https://doi.org/10.1128/jvi.02490-07> PMID: 18287233
52. Thézé J, Bézier A, Periquet G, Drezen J-M, Herniou EA. Paleozoic origin of insect large dsDNA viruses. *Proc Natl Acad Sci U S A*. 2011; 108(38):15931. <https://doi.org/10.1073/pnas.1105580108> PMID: 21911395
53. Bézier A, Annaheim M, Herbinière J, Wetterwald C, Gyapay G, Bernard-Samain S, et al. Polydnaviruses of braconid wasps derive from an ancestral nudivirus. *Science*. 2009; 323(5916):926–930. <https://doi.org/10.1126/science.1166788> PMID: 19213916
54. Finlay BB, McFadden G. Anti-immunology: evasion of the host immune system by bacterial and viral pathogens. *Cell*. 2006; 124(4):767–782. <https://doi.org/10.1016/j.cell.2006.01.034> PMID: 16497587
55. Peng K, van Lent JWM, Boeren S, Fang M, Theilmann DA, Erlandson MA, et al. Characterization of novel components of the baculovirus *per os* infectivity factor complex. *J Virol*. 2012; 86(9):4981–4988. <https://doi.org/10.1128/JVI.06801-11> PMID: 22379094
56. Ito K, Kidokoro K, Sezutsu H, Nohata J, Yamamoto K, Kobayashi I, et al. Deletion of a gene encoding an amino acid transporter in the midgut membrane causes resistance to a *Bombyx parvo-like virus*. *Proc Natl Acad Sci U S A*. 2008; 105(21):7523–7527. <https://doi.org/10.1073/pnas.0711841105> PMID: 18495929
57. Lane RK, Guo H, Fisher AD, Diep J, Lai Z, Chen Y, et al. Necroptosis-based CRISPR knockout screen reveals Neuropilin-1 as a critical host factor for early stages of murine cytomegalovirus infection. *Proc Natl Acad Sci U S A*. 2020; 117(33):20109. <https://doi.org/10.1073/pnas.1921315117> PMID: 32747526
58. Hilleman MR. Strategies and mechanisms for host and pathogen survival in acute and persistent viral infections. *Proc Natl Acad Sci U S A*. 2004; 101(suppl 2):14560–14566. <https://doi.org/10.1073/pnas.0404758101> PMID: 15297608
59. Younis S, Kamel W, Falkeborn T, Wang H, Yu D, Daniels R, et al. Multiple nuclear-replicating viruses require the stress-induced protein ZC3H11A for efficient growth. *Proc Natl Acad Sci U S A*. 2018; 115(16):E3808–E3816. <https://doi.org/10.1073/pnas.1722333115> PMID: 29610341
60. Xu W, Kong X, Liu H, Wang H, Wu X. *Bombyx mori* nucleopolyhedrovirus F-like protein Bm14 is a type I integral membrane protein that facilitates ODV attachment to the midgut epithelial cells. *J Gen Virol*. 2020; 101(3):309–321. <https://doi.org/10.1099/jgv.0.001389> PMID: 32003710
61. Sander JD, Maeder ML, Reyon D, Voytas DF, Joung JK, Dobbs D. ZiFiT (Zinc Finger Targeter): an updated zinc finger engineering tool. *Nucleic Acids Res*. 2010; 38:W462–468. <https://doi.org/10.1093/nar/gkq319> PMID: 20435679
62. Gao Y, Liu YC, Jia SZ, Liang YT, Wang HB. Imaginal disc growth factor maintains cuticle structure and controls melanization in the spot pattern formation of *Bombyx mori*. *PLoS Genet*. 2020; 16(9):e1008980. <https://doi.org/10.1371/journal.pgen.1008980> PMID: 32986708
63. Yu Z, Ren M, Wang Z, Zhang B, Rong YS, Jiao R, et al. Highly efficient genome modifications mediated by CRISPR/Cas9 in *Drosophila*. *Genetics*. 2013; 195(1):289–291. <https://doi.org/10.1534/genetics.113.153825> PMID: 23833182
64. Wang Y, Li Z, Xu J, Zeng B, Ling L, You L, et al. The CRISPR/Cas system mediates efficient genome engineering in *Bombyx mori*. *Cell Res*. 2013; 23(12):1414–1416. <https://doi.org/10.1038/cr.2013.146> PMID: 24165890
65. Wei W, Xin H, Roy B, Dai J, Miao Y, Gao G. Heritable genome editing with CRISPR/Cas9 in the silkworm, *Bombyx mori*. *PLoS One*. 2014; 9(7):e101210. <https://doi.org/10.1371/journal.pone.0101210> PMID: 25013902